Bistable Switching between Low and High Absorbance States in Oleate-Capped PbS Quantum Dots

Mark J. Fernée,* Peter Jensen, and Halina Rubinsztein-Dunlop

Centre for Quantum Computer Technology, School of Physical Sciences, The University of Queensland, Queensland 4072, Australia

ABSTRACT We report hysteretic photophysical behavior over a 110 K temperature range in freshly prepared colloidal suspensions of PbS/oleic acid nanocrystals. A bistable regime consisting of both low and high absorbance states of the PbS nanocrystals is observed between 215 and 240 K. The change in absorbance is significant (increasing by at least a factor of 5) and is shown to be entirely nonexcitonic in origin. The absorbance change is correlated with a thermal hysteresis in the photoluminescence quenching rate associated with a sudden switching of the quenching behavior upon cooling below 220 K. Most surprisingly, these effects are temporary, resulting in either the complete destruction of the smallest nanocrystals or stabilization of the larger nanocrystals after many weeks. We attribute this anomalous behavior to a structural phase change in the oleate surface ligands. This phenomenon thus illustrates the potentially large effect that surfaces can have on photophysical properties of PbS nanocrystals. Furthermore it opens up the possibility of surface engineering the photophysical properties of these materials for different applications such as photovoltaics.

KEYWORDS: PbS nanocrystals · quantum dots · bistability · photoluminescence quenching · surface effects · phase change

Lead salt nanocrystals (NCs) are an interesting class of quantum dot materials because of their potential for tunable emission in the mid- to near-IR.[1,2] Since the first report of widely size tunable PbSe NCs,[3] there has been a growing interest in these materials. Size tunable syntheses were also reported for PbS[4,5] and PbTe NCs[1,6,7] with distinct band-edge excitonic absorption features that followed theoretical expectation.[8] Alternative surface treatments have been reported and used to demonstrate electroluminescence,[9,10] OLEDs,[11,12] and water-soluble NCs for biological applications.[13] Furthermore, carrier multiplication[14−19] has been vigorously explored for efficient photovoltaic applications.[12,20,21]

The first reports of a synthesis for colloidal PbS NCs[22,23] were followed by many different syntheses reporting confusing and often contradictory photophysical behavior.[24−28] The first report of a well-controlled size-tunable colloidal synthesis was that of Hines and Scholes.[4] This synthesis produced NCs that displayed a clearly identifiable excitonic absorption peak. Prior to this synthesis, the only consistent size-tunable synthesis that exhibited a clear excitonic absorption peak was in various glasses.[29,30] Earlier syntheses either resulted in a rather featureless spectra[24−28] or a curious three-peaked spectrum[23,31] that has never been clearly proven as of excitonic origin. It has been postulated that the difficulty in achieving absorption spectra of clear excitonic origin is due to strong surface interactions.[24−27]

Even with the current high quality syntheses, the photophysical properties of lead salt NCs still retain significant uncertainties. For example, the photoluminescence lifetimes have been found to be unusually long, which was first attributed to dielectric screening of the transition dipole.[32] However, these materials can also exhibit a large Stokes shift of the emission. This Stokes shift has been attributed to surface state-induced trapping of one of the charge carriers,[33] which could also account for the long lifetime. However, recent modeling of PbSe NCs indicate the absence of trap states within the band gap and has attributed the Stokes shift to Franck−Condon relaxation,[34] resulting from highly strained surfaces in small NCs. Curiously, it was reported that control of the shell layer growth in PbSe/PbS core/shell NCs could modify and even remove the Stokes shift entirely.[35] Efficient carrier relaxation was also found in PbSe NCs,[32] contrary to expectations that the Auger relaxation route would be inefficient in these materials. Efficient relaxation was recently explained in terms of a large increase in the state density due to the 4-fold degenerate L-valley band gap, which prevents a phonon bottleneck.[36] Other properties, such as extremely large room temperature emission linewidths and strong acoustic phonon coupling have

*Address correspondence to fernee@physics.uq.edu.au.

Received for review May 27, 2009 and accepted August 07, 2009.

Published online August 12, 2009. 10.1021/nn9005544 CCC: $40.75

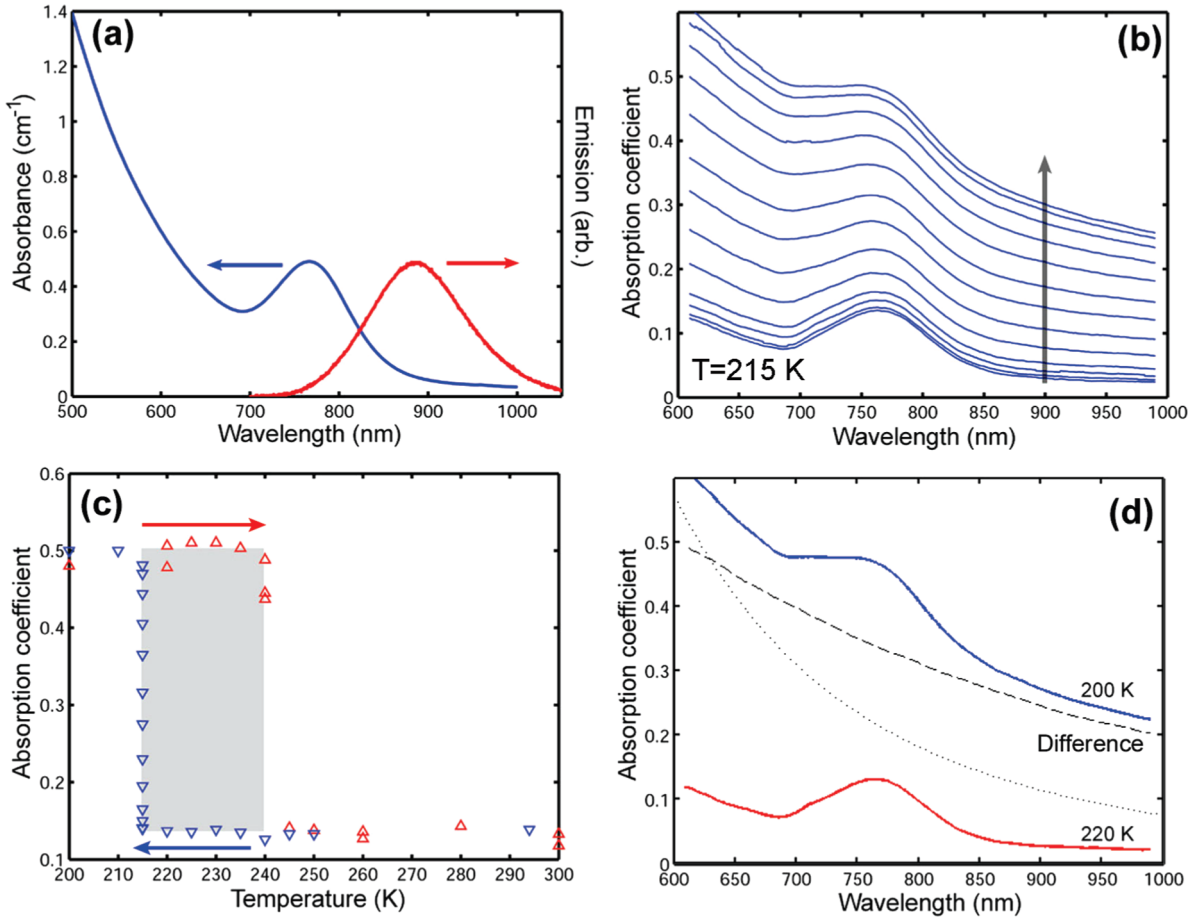

Figure 1. Absorption properties: (a) typical room temperature absorption and emission from a colloidal solution of oleic acid capped PbS NCs dispersed in heptane; (b) 13 successive absorption spectra obtained at a temperature of 215 K over 60 min; (c) thermal hysteresis in the absorption with switching at 215 K and ~240 K (cooling, blue lower triangles; warming, red upper triangles); (d) comparison of the absorption on either side of the transition at 215 K. The change in absorbance is also indicated (dashed) and a curve indicating a $1/\lambda^4$ Rayleigh scattering dependence is also included for comparison (dotted).

been predicted[37] and observed.[38,39] Efficient photoluminescence up-conversion has also been observed at both room temperature[40] and at cryogenic temperatures.[41] Of all the properties mentioned above, some have been attributed to surface effects, while others to intrinsic exciton properties. However it may be difficult to unravel the influence of one from the other.

Recent simulations have implicated surface charges in modifying the spectra associated with PbSe NCs.[42] It was predicted that surface charges can attenuate both the absorption and emission properties of the NCs. Here we report large changes in both absorption and emission in oleic acid capped PbS NCs over a 110 K variation in temperature. These changes manifest as bistable absorption and emission spectra and are attributed to changes in the surface ligand structure. These results illustrate the dramatic effect that the surface has on the photophysical properties of PbS NCs.

RESULTS AND DISCUSSION

Absorbance Hysteresis. We undertake a low temperature study of the optical properties of PbS NCs dispersed as a colloidal suspension in *n*-heptane, allowing a temperature range from 190 to 300 K to be investigated as a liquid colloid. This study was prompted by curious visible changes in the color of a solution of the smallest sized (~1 nm diameter)[5] PbS NCs that was stored in a freezer. The effects reported here were present in all freshly prepared samples of PbS NC colloids across the entire size range used in this study (1−3 nm diameter PbS NCs).[38] The PbS NCs were synthesized using a low temperature variant of the Hines and Scholes procedure, which has been reported elsewhere.[36]

A room temperature absorption and emission spectrum obtained from a PbS NC colloidal solution are shown in Figure 1a, indicating a narrow size distribution and predominantly band-edge PL. The large Stokes shift of the PL is typical of PbS NCs in this size range exhibiting strong quantum confinement.[33] Upon lowering the temperature of the solution we find the absorption switches between a low absorbing state and a high absorbing state (Figure 1b). This switch occurs slowly at 215 K over the course of nearly an hour, and all spectra obtained below this temperature exhibit this increased absorbance. In fact we find that there are

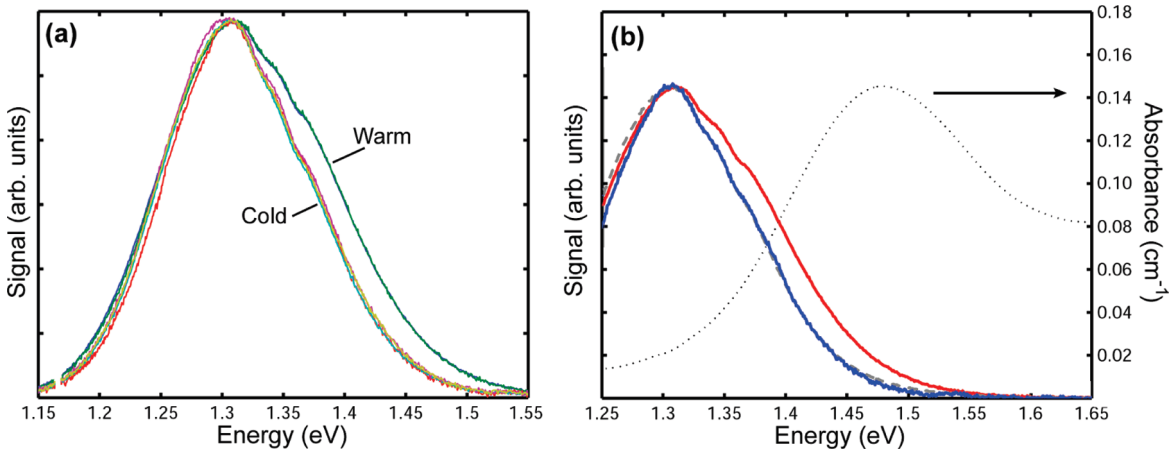

Figure 2. Reabsorption of PL: (a) series of 6 PL spectra (normalized by peak height) obtained while warming from ~200 K; (b) warm (red) and cold (blue) PL spectra overlaid with a warm PL spectrum adjusted using a reabsorption model (gray dashed) treating an order of magnitude increase in the PbS NC absorbance. The room temperature absorbance used in the model is indicated (dotted).

two distinct absorbing states and that over a wide temperature region these two states are bistable. In Figure 1c, we show that the switch between the low absorbing state and the high absorbing state depends on the direction in which the temperature is varied. When raising the temperature, the switch appears around 240 K, compared to the 215 K switch when lowering the temperature. The nature of the change, determined by taking the difference in the spectra from the low and high absorbing state in Figure 1d, has no component from the band-edge exciton. However, the change is clearly increasing with decreasing wavelength, (the dependence is approximately linear with frequency). In contrast we provide a curve following a quartic frequency dependence characteristic of elastic Rayleigh scattering, which clearly does not fit the observed change.

The extent of the change is indicated in Figure 2 using the PL from the PbS NCs to monitor the absorption change near the PbS NC band-edge. Here the large Stokes shift of the PL is useful in that it allows us to monitor the change at and beyond the absorption band-edge. This data was taken using a standard quartz cuvette with a 10 mm square cross-section. The cuvette was first cooled in dry ice and then allowed to slowly warm while successive spectra were taken. The laser beam was passed through the center of the cuvette and the PL monitored from the side with ~5 mm reabsorption path length. We find that the spectra comprise only two dominant spectral shapes that strongly differ on the high energy side, as shown in Figure 2a. In Figure 2b we plot a warm and cold PL spectrum. The cold spectrum is nearly perfectly overlaid with a spectrum that is derived from the warm spectrum after simulating increased reabsorption estimated by multiplying the room temperature absorbance by a factor of 10. The fact that the reabsorption model closely reproduces the cold spectrum indicates that the absorption change is limited to energies above the PbS band-edge.

Photoluminescence Hysteresis. The large temperature hysteresis in absorption prompts us to look for evidence of this change in the PL properties. In Figure 3a we show photoluminescence excitation (PLE) spectra obtained at 190 and 300 K. A difference curve indicates the change involves the band-edge exciton resonance, in contrast to the change observed in absorption in Figure 1d. While the PL exhibits large changes in the integrated emission over the 190−300 K temperature range (as shown in Figure 3b), this change shows no sign of the sharp switching that we observe in the absorption properties. This confirms that the changes we find in absorption are not of excitonic origin, nor do they significantly affect or modify the excitonic transition. The large change in PL-integrated intensity (total emission) is fit with a curve of the form, $I = I_0(1 - e^{-\beta/T+\gamma})$, suggesting a process of thermally activated PL quenching.[43] This indicates a temperature dependent trap-state density. A plot of both warming and cooling cycles between 190 and 300 K, using an Arrhenius-type plot of $\ln(1 - I/I_0)$ *vs* $1/T$, reveals a thermal hysteresis. However the nature of this hysteresis is different to that found for absorption, as it extends over the entire temperature range. With decreasing temperature, the rate of PL recovery is far greater than PL quenching rate on warming for most of the range. However, on cooling toward the lowest temperatures, the PL recovery switches to a regime of anomalous PL quenching from 220 to 190 K. This is close to the 215 K absorption switching point and indicates a similarly abrupt change in the physical properties of the system. We show that a thermal steady-state was achieved for each measurement by the fact that the thermal hysteresis is not apparent in the plot of the PL spectral line width as a function of temperature in Figure 3d (using the line width as an effective thermometer).[39] Thus the hysteresis in Figure 3c is not an artifact. The lack of a hysteresis in the line width dependence also shows that the changes are not reflected in the excitonic prop-

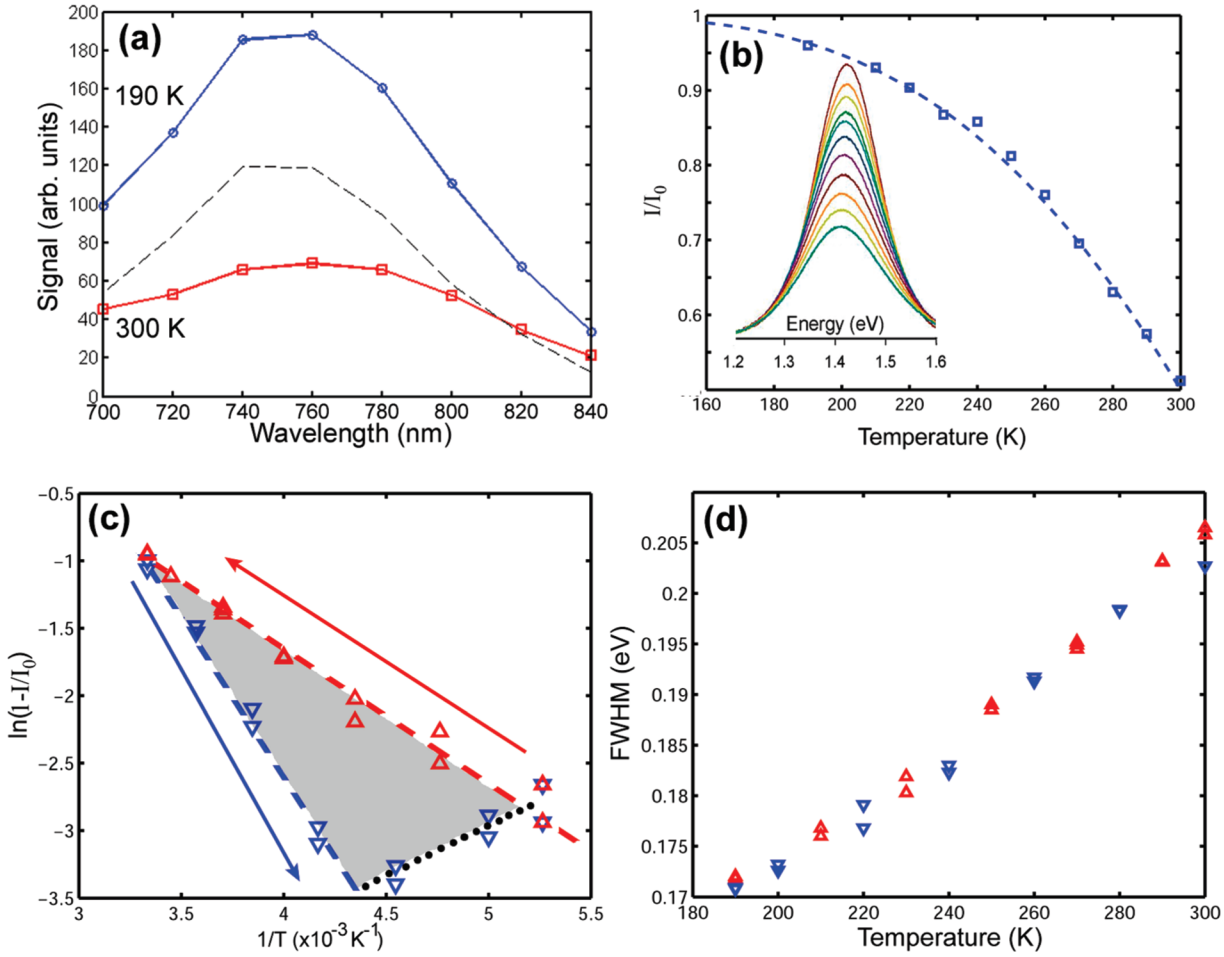

Figure 3. PL properties: (a) PLE spectra obtained at 190 K (blue circles) and 300 K (red squares). A difference curve is also indicated (dashed). (b) Variation of the integrated PL intensity as a function of temperature, obtained using 2 mW pump power at 760 nm resonant with the excitonic absorption peak. The integrated intensity normalized to a saturation parameter is described in the text. A fit to a thermal activation curve is also included (dashed). (Inset: the individual spectra used to generate the graph). Nonresonant 532 nm 1.5 mW pump results, (c—d). (c) An Arrhenius-type plot revealing the thermal activation rates for heating (upper red triangles) and cooling (lower blue triangles). Straight lines are provided as a guide to the eye. (d) A plot of the PL fwhm as a function of sample temperature. Data points from the heating cycle (upper red triangles) and cooling cycle (lower blue triangles) are distinguished.

erties, which have been shown to predominantly determine the PL line width.[39]

Transient Response. Different transient responses of the system are also studied to gain further insight. In Figure 4a we plot the change in the absorption measured at the band-edge exciton peak on cooling the system. Three different cooling rates are shown and arrows indicate the approximate position when the system has crossed the 215 K switching point shown in Figure 1b. Cooling was stopped at 190 K to prevent freezing the sample. Here we see that the change occurs slowly, independent of the cooling rate. In all cases the absorption first decreases before slowly increasing. In contrast, the behavior upon heating exhibits a marked dependency on the heating rate. However all traces indicate a transition to a highly absorbing intermediate state prior to switching to the low absorbing state. Arrows mark the 240 K transition temperature indicating the transition to the transient high absorbing state starts well before the switching temperature is reached. In fact the slowest heating rate clearly indicates that the high absorbing transient occurs before the switch temperature determined in Figure 1c. PL transients were also investigated. PL was measured at the maximum emission. In Figure 4c we show the effect of cooling on the PL. Here we see an initial period consistent with the recovery of the PL quantum yield with decreasing temperature, then a sudden switch to the opposite behavior. For heating we see first an initial drop in PL consistent with the existence of the high absorbing transient state in Figure 4b. This dip cannot be attributed to reabsorption of the PL, as will be discussed below, but indicates a region of reduced quantum yield. Even though there are large absorption changes in the system, we can show that the PL properties are only slightly affected by reabsorption due partly to the large Stokes shift of the PL from the band-edge along with the geometry of the narrow 2 mm thick cuvette. Evidence for minimal reabsorption in this geometry can be found in Figure 3b, where only a slight reduction in the PL signal is evident in the low-temperature high-absorbance regime. Furthermore, that the decrease in

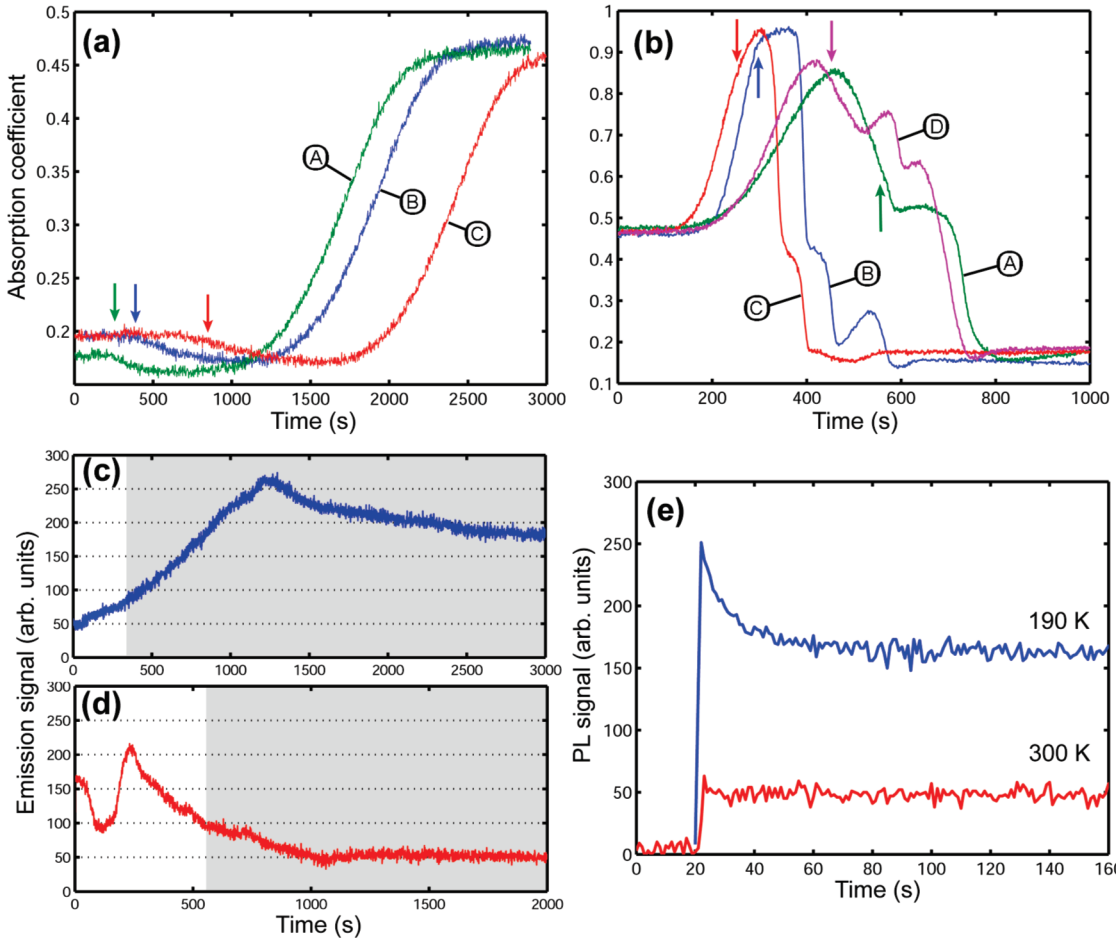

Figure 4. Transient response: (a) Absorption measured at the exciton peak at 760 nm during rapid cooling from 300 to 190 K. Cooling rates are approximately −20, −10, and −5 K/min for A, B, and C, respectively. Arrows mark the 215 K switching temperature. (b) Absorption measured at the exciton peak at 760 nm during rapid heating from 190 to 300 K. Heating rates are 4.5, 12, 12, and 7.5 K/min for A, B, C, and D, respectively. Curve B is temporally offset due to lower starting temperature (181 K). Arrows mark the 240 K switching temperature. (c−e) PL emission measured at the exciton peak at 860 nm using 0.5 mW 532 nm pump laser: (c) rapid cooling from 300 to 190 K at *ca.* −20 K/min; (d) rapid heating from 190 to 300 K at ∼12 K/min (note: the shaded regions indicate the cessation of cooling/heating in panels c and d, respectively); (e) response to sudden illumination at 190 and 300 K.

PL seen in the right-hand side of Figure 4c is not attributable to reabsorption is demonstrated in Figure 4e, where we see that the highest PL signal seen in Figure 4c can be recovered in the transient response to the sudden application of the pump laser at 190 K. This response is absent at 300 K and is indicative of the change in the system at low temperatures. Thus the high absorbing state is associated with a photoactivated PL quenching process.

Laser Scatter. The 532 nm pump beam throughput was monitored on a screen using a video camera during the cooling and warming cycles in order to monitor scattering from the sample. Visually, the laser spot appeared unchanged during the cool-down phase and we present a comparison of the laser beam profile at both extremes of the temperature range in Figure 5a. In the high absorption regime at 190 K there is ∼50% reduction in the throughput beam intensity. However, as we show in Figure 5a, this lost pump intensity is not detected as scattered light as there is no detectable additional intensity on either side of the laser spot. This is consistent with the observation that the solution remains an optically clear liquid at 190 K. We note that a region of strong laser scattering is encountered during warming (see Figure S4 and S5 in Supporting Information), which can be understood as an inhomogeneous regime containing a mixture of both high and low absorbance domains, resulting in strong Mie scattering. In Figure 5b we show the scattered 532 nm pump collected with the PL signal (using the grating second-order reflection). Here we clearly see there is an order of magnitude reduction in the scattered signal at 190 K, consistent with a large increase in absorbance. In contrast to the strong reduction in pump scatter, the PL signal increases (as indicated in Figure 3), which is indicative of an absorbance change *above* the PbS band-edge (as shown in Figure 2).

In the configuration with the laser incident at 45 deg to the face of the cuvette, a shift in the laser spot (Figure 5c insert) between the 190 and 300 K operation

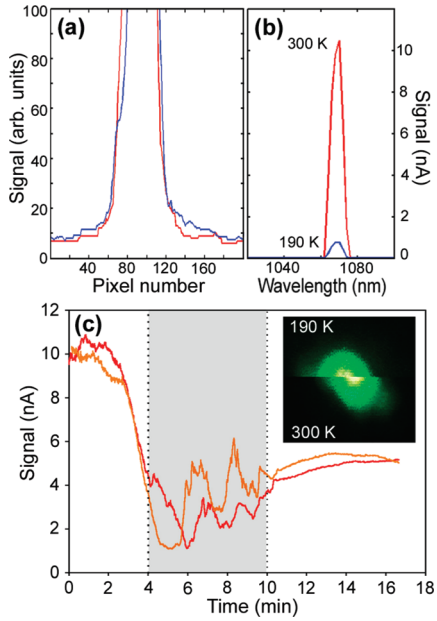

Figure 5. Laser scatter: (a) cross section of the throughput laser spot at both 190 K (blue) and 300 K (red) (note that the 190 K profile has been aligned with the 300 K to account for an observed shift); (b) scattered 532 nm pump collected with the PL signal at 90 degrees to the pump propagation direction; (c) monitoring the intensity at the 190 K laser spot maximum. The sample is heated from 190 to 300 K at a rate of 12 K/min. The shaded region corresponds to a region of strong scattering. (Inset: Comparison of the 190 and 300 K laser beam profiles showing displacement of the beam.)

is apparent, indicative of a refractive index change between the two temperature regimes. In Figure 5c we monitor the peak of the laser spot at 190 K using a silicon photodiode with a small aperture in front in order to sample only a small section of the beam. We see a sudden and abrupt change upon heating the sample from 190 K, with the change correlated to the onset of the absorbance change as shown in curve B of Figure 4b (where the same heating rate and start temperature are used). A strong scattering regime is highlighted by the shaded section. Here the reduced signal at 300 K is indicative of the beam displacement so that a point on the side of the beam profile is now detected (which is lower than the peak intensity). The observation of an abrupt refractive index change correlated with the abrupt absorption change indicates the change is in the bulk of the sample and not an interface or surface effect.

In general, effects evident in the PL properties of the system are indicative of changes to the NCs. Here we correlate large changes in absorbance with changes in the PL properties. In both cases a thermal hysteresis is found. The changes in absorbance indicate the presence of both a low absorbance, mostly excitonic state, and a high absorbance, mostly nonexcitonic state, with a wide region of bistability. These changes in absorbance are correlated to changes in the PL quenching rate, which also exhibits a thermal hysteresis. The hysteresis in PL quenching rates indicates that the switch to the high absorbance state results in increased PL quenching. If we relate PL quenching to the presence of surface traps, then the two different rates for PL quenching and PL recovery shown in Figure 3c indicate that there is an abrupt increase in the surface trap density as the temperature is reduced below the 215 K switching threshold. This abrupt increase in the number of surface traps lowers the PL recovery rate with increasing temperature, resulting in the thermal hysteresis between the trap activation rate and the trap deactivation rate. In addition, the transient response of the PL to sudden illumination shown in Figure 4e suggests that the increased surface trap density is not thermally activated, but photophysically activated.

While we can show that the large absorbance change is reflected in changes to the PL properties, we also see that the high absorbance state is nonexcitonic with a zero quantum yield, as the hysteresis evident in Figure 1c is not seen as an abrupt change in PL as shown in Figure 3b. It is interesting that the high absorbance state is additive to, but unperturbing of the excitonic state, indicating very little coupling between the two states. Thus the radiative quantum yield of the *excitonic* state (if we neglect the additive nonexcitonic absorption) is barely affected. However, the transient response to heating indicates a transient absorbing regime correlated with dramatically reduced quantum yield of the excitonic component, as evidenced in Figure 4d.

Overall the exact nature of the change that takes place remains speculative. We can exclude many trivial possibilities, such as solvent contraction effects, an increased freezing point for the colloidal suspensions, and NC aggregation as follows: First, the increase in absorbance is purely nonexcitonic, which rules out simple concentration changes such as a solvent contraction effect, which should proportionally increase the entire absorption spectrum. We observed the solution at all operating temperatures and found it to be an optically clear liquid. There was also no noticeable increase in laser scatter through the solution at the lowest operating temperature, supporting the above observation that the solution is maintained above its freezing point. Aggregation of the NCs would be expected to either increase laser scattering for large aggregates, or result in some modification of the PL properties through coupling between NCs.[44] The plot of PL line width as a function of temperature (Figure 3d) shows no indication of any sudden change, which should signify the aggregation. One final and very important property that can be used in the identification of the nature of the change is that the effect itself is only temporary. The larger NCs, such as those used to provide the data for this report, eventually stabilize over a period of between 2 weeks and a month, no longer exhibiting the properties described here, but retaining the sharp exciton peak. More

dramatically, the smallest PbS NCs completely destabilize after as few as three thermal cycles and reform as a red polydisperse PbS NC colloid devoid of any sharp excitonic peak. Such a dramatic effect indicates that the change is directly related to the NCs and not the surrounding matrix. Furthermore, there is evidence that the absorbance change is dependent on the size of the NCs as the small 1 nm PbS NCs changed absorbance state upon cooling to a significantly higher temperature (see Figure S3, Supporting Information).

The correlation between PL and absorption changes and the identification of the nature of the change in PL properties points to the surface of the NC as the location of the change. These changes are also only found in colloidal solutions. PbS NCs deposited into PMMA polymer films do not exhibit the properties described here (see Figure S6, Supporting Information). Thus we are able to speculate on the nature of the phenomenon as a change in the configuration of the surface ligands that switches between predominantly excitonic absorption and a highly absorbing nonexcitonic state. Similar phase changes in the surface ligands have been found in CdSe NCs,[45] marking the transition between a quenching and antiquenching regime. This was attributed to the emergence of a rotational degree of freedom.[45,46] Studies of oleate self-assembled monolayers also show a well ordered closely packed structure,[47] indicating a similar phase transition may be possible. Curiously this rotational phase change[46] occurs at a temperature close to what is reported here, hinting at a similar origin. However, such phase changes do not explain the bistability, although these models do not include the spherical/faceted topology. Furthermore, the temporary nature of the effect in PbS NCs suggests that the ligand configuration may be a result of the low temperature synthesis that does not effectively anneal the surface ligands into a global minimum energy state. Nevertheless, the behavior reported here serves to illustrate the large effect that the surface can have on these materials and may help explain some of the anomalous results obtained from other syntheses of PbS NCs such as those that result in featureless absorption spectra in spite of a narrow size distribution.[24−28]

CONCLUSIONS

We find a pronounced thermal hysteresis in the absorbance of colloidal suspensions of oleic acid capped PbS NCs that we attribute to a structural phase change in the surface capping ligands. The increase in absorbance can be extremely large (we report a factor of 5) and is entirely nonexcitonic in nature, highlighting the huge effect that surface changes can have on these materials. Thus two absorption regimes are revealed: An excitonic and a nonexcitonic regime. The change in the absorbing state is reflected in the emission properties by an abrupt increase in PL quenching, which results in a thermal hysteresis in the PL quenching rate. Once more, we find the changes to the PL properties are entirely nonexcitonic in nature, consistent with a change in the surface properties. These surface-induced changes to the optical properties of PbS NC colloids offer some explanation for the wide variation in optical properties observed between PbS NC colloids prepared using different synthetic routes. If they can be stabilized, novel surface states in PbS NCs may ultimately be useful in applications such as photovoltaics due to their high absorbance and low PL quantum yield.

Overall, understanding the effect of the surface on NC materials is crucial for any potential application. The observation of a large nonexcitonic absorption has important consequences for many technological applications of these materials, such as a potential loss of luminescence quantum yield in OLED and laser applications as well as providing a misleading optical cross-section in photovoltaic and photodetector applications.

METHODS

The synthesis of the oleic acid capped PbS NCs used in these experiments has been described elsewhere.[39] Briefly, the reaction was conducted in 25 mL Erlenmeyer flasks fitted with rubber septa and containing a magnetic stirrer bar. A stock lead oleate solutions were prepared by mixing 0.1 g of lead acetate (AR grade) with 0.4 mL of oleic acid and 9.6 mL of *n*-decane. The solutions were heated to 130 °C for 30 min with moderate stirring under a continuous flow of Ar. The precursor solution was then cooled to the appropriate reaction temperature between 50 and 80 °C in a water bath. With vigorous stirring, 1 mL of H_2S gas is injected slowly over 10 s. The reaction is allowed to proceed for between 90 and 150 s. Because of the low temperature, the reaction was effectively stopped at the appropriate time with the injection of 4-fold excess of *n*-heptane that had been cooled in a freezer. The solutions were then centrifuged to remove any precipitates. The NCs were then precipitated from the supernatant by adding methanol until the solution went cloudy, then centrifuging and discarding the supernatant. The oleic acid capped PbS NCs were then redissolved in *n*-heptane, stored in a flask wrapped in aluminum foil, and kept in a refrigerator for 48 h to allow natural focusing of the size distribution before further study.

Absorption characterization of each solution was conducted at room temperature using a standard absorption spectrometer (Perkin-Elmer, Lambda 40). Cryogenic measurements were conducted using a liquid-nitrogen-cooled optical cryostat (Oxford microstat-N). Small cuvettes with a 2 mm spacing between optical windows were made from two coverslips appropriately spaced with epoxy resin side walls (see Figure S1, Supporting Information). The cuvettes were filled with solutions of oleic acid capped PbS NCs in *n*-heptane were mounted on the coldfinger.

Low temperature absorption measurements were conducted using light from a tungsten reference lamp, filtered with a 550 nm low pass filter and passed through a 300 mm scanning monochromator (Acton 300i). The output was collimated and passed through the sample and focused onto a large area silicon photodiode (see schematic Figure S2, Supporting Information). A relative zero absorbance baseline signal was measured using a cuvette filled with *n*-heptane and used to generate subsequent absorption spectra.

Low temperature photoluminescence (PL) measurements were conducted using either a 532 nm laser light or tunable cw emission from a Ti:sapphire laser around 800 nm. The samples were mounted in the cryostat with the cuvettes at 45° to the laser. The PL emission was collected with a $f = 100$ mm lens and coupled into a 300 mm scanning spectrometer (Acton 300i) fitted with a silicon photodiode. The pump powers were kept at or below 2 mW, and operation in the linear pump regime was verified.

Acknowledgment. This work was financially supported by the Australian Research Council.

Supporting Information Available: Details of the experimental apparatus including cuvette manufacture. Observation of pump beam scattering transient with increasing temperature. Absorption results obtained in PMMA films. A visual indication of absorbance change in 1 nm diameter PbS NC solutions. This material is available free of charge *via* the Internet at http://pubs.acs.org.

REFERENCES AND NOTES

1. Rogach, A. L.; Eychmuller, A.; Hickey, S. G.; Kershaw, S. V. Infrared-Emitting Colloidal Nanocrystals: Synthesis, Assembly, Spectroscopy, and Applications. *Small* **2007**, *3*, 536–557.
2. Sargent, E. H. Infrared Quantum Dots. *Adv. Mater.* **2005**, *17*, 515–522.
3. Murray, C. B.; Sun, S. H.; Gaschler, W.; Doyle, H.; Betley, T. A.; Kagan, C. R. Colloidal Synthesis of Nanocrystals and Nanocrystal Superlattices. *IBM J. Res. Dev.* **2001**, *45*, 47.
4. Hines, M. A.; Scholes, G. D. Colloidal PbS Nanocrystals with Size-Tunable Near-Infrared Emission: Observation of Post-Synthesis Self-Narrowing of the Particle Size Distribution. *Adv. Mater.* **2003**, *15*, 1844.
5. Warner, J. H.; Thomsen, E.; Watt, A. R.; Heckenberg, N. R.; Rubinsztein-Dunlop, H. Time-Resolved Photoluminescence Spectroscopy of Ligand-Capped PbS Nanocrystals. *Nanotechnology* **2005**, *16*, 175–179.
6. Urban, J. J.; Talapin, D. V.; Shevchenko, E. V.; Murray, C. B. Self-Assembly of PbTe Quantum Dots into Nanocrystal Superlattices and Glassy Films. *J. Am. Chem. Soc.* **2006**, *128*, 3248–3255.
7. Mokari, T. L.; Zhang, M. J.; Yang, P. D. Shape, Size, and Assembly Control of PbTe Nanocrystals. *J. Am. Chem. Soc.* **2007**, *129*, 9864.
8. Kang, I.; Wise, F. W. Electronic Structure and Optical Properties of PbS and PbSe Quantum Dots. *J. Opt. Soc. Am. B* **1997**, *14*, 1632–1646.
9. Bakueva, L.; Musikhin, S.; Hines, M. A.; Chang, T. W. F.; Tzolov, M.; Scholes, G. D.; Sargent, E. H. Size-Tunable Infrared (1000−1600 nm) Electroluminescence from PbS Quantum-Dot Nanocrystals in a Semiconducting Polymer. *Appl. Phys. Lett.* **2003**, *82*, 2895–2897.
10. Bourdakos, K. N.; Dissanayake, D. M. N. M.; Lutz, T.; Silva, S. R. P.; Curry, R. J. Highly Efficient Near-Infrared Hybrid Organic−Inorganic Nanocrystal Electroluminescence Device. *Appl. Phys. Lett.* **2008**, *92*, 153311.
11. Steckel, J. S.; Coe-Sullivan, S.; Bulovic, V.; Bawendi, M. G. 1.3 to 1.55 μm Tunable Electroluminescence from PbSe Quantum Dots Embedded Within an Organic Device. *Adv. Mater.* **2003**, *15*, 1862.
12. Konstantatos, G.; Huang, C. J.; Levina, L.; Lu, Z. H.; Sargent, E. H. Efficient Infrared Electroluminescent Devices Using Solution-Processed Colloidal Quantum Dots. *Adv. Funct. Mater.* **2005**, *15*, 1865–1869.
13. Hyun, B. R.; Chen, H. Y.; Rey, D. A.; Wise, F. W.; Batt, C. A. Near-Infrared Fluorescence Imaging With Water-Soluble Lead Salt Quantum Dots. *J. Phys. Chem. B* **2007**, *111*, 5726–5730.
14. Schaller, R.; Klimov, V. High Efficiency Carrier Multiplication in PbSe Nanocrystals: Implications For Solar Energy Conversion. *Phys. Rev. Lett.* **2004**, *92*, 186601.
15. Ellingson, R. J.; Beard, M. C.; Johnson, J. C.; Yu, P. R.; Micic, O. I.; Nozik, A. J.; Shabaev, A.; Efros, A. L. Highly Efficient Multiple Exciton Generation in Colloidal PbSe and PbS Quantum Dots. *Nano Lett.* **2005**, *5*, 865.
16. Klimov, V. Detailed-Balance Power Conversion Limits of Nanocrystal-Quantum-Dot Solar Cells in the Presence of Carrier Multiplication. *Appl. Phys. Lett.* **2006**, *89*, 123118.
17. Trinh, M. T.; Houtepen, A. J.; Schins, J. M.; Hanrath, T.; Piris, J.; Knulst, W.; Goossens, A. P. L. M.; Siebbeles, L. D. A. In Spite of Recent Doubts Carrier Multiplication Does Occur in PbSe Nanocrystals. *Nano Lett.* **2008**, *8*, 1713–1718.
18. Beard, M. C.; Midgett, A. G.; Law, M.; Semonin, O. E.; Ellingson, R. J.; Nozik, A. J. Variations in the Quantum Efficiency of Multiple Exciton Generation for a Series of Chemically Treated PbSe Nanocrystal Films. *Nano Lett.* **2009**, *9*, 836–845.
19. Murphy, J. E.; Beard, M. C.; Norman, A. G.; Ahrenkiel, S. P.; Johnson, J. C.; Yu, P. R.; Micic, O. I.; Ellingson, R. J.; Nozik, A. J. PbTe Colloidal Nanocrystals: Synthesis, Characterization, and Multiple Exciton Generation. *J. Am. Chem. Soc.* **2006**, *128*, 3241–3247.
20. McDonald, S. A.; Konstantatos, G.; Zhang, S. G.; Cyr, P. W.; Klem, E. J. D.; Levina, L.; Sargent, E. H. Solution-Processed PbS Quantum Dot Infrared Photodetectors and Photovoltaics. *Nat. Mater.* **2005**, *4*, 138.
21. Sargent, E. H. Solar Cells, Photodetectors, and Optical Sources from Infrared Colloidal Quantum Dots. *Adv. Mater.* **2008**, *20*, 3958–3964.
22. Gallardo, S.; Gutierrez, M.; Henglein, A.; Janata, E. Photochemistry and Radiation-Chemistry of Colloidal Semiconductors 34 Properties of Q-PbS. *Ber. Bunsen-Ges. Phys. Chem.* **1989**, *93*, 1080.
23. Nenadovic, M. T.; Comor, M. I.; Vasic, V.; Micic, O. I. Transient Bleaching of Small PbS Colloids—Influence of Surface-Properties. *J. Phys. Chem.* **1990**, *94*, 6390.
24. Guo, L.; Wu, Z. H.; Ai, X. C.; Li, Q. S.; Zhu, H. S.; Yang, S. H. The Influence of Surface Modification on the Femtosecond Optical Kerr Effect of PbS Nanoparticles. *Opt. Mater.* **2000**, *14*, 247.
25. Guo, L.; Ibrahim, K.; Liu, F. Q.; Ai, X. C.; Li, Q. S.; Zhu, H. S.; Zou, Y. H. Transient Optical Properties of Novel PbS Nanoparticles Coated with 2,6-O-diallyl-beta-CD. *J. Lumin.* **1999**, *82*, 111.
26. Patel, A. A.; Wu, F. X.; Zhang, J. Z.; Torres-Martinez, C. L.; Mehra, R. K.; Yang, Y.; Risbud, S. H. Synthesis, Optical Spectroscopy, and Ultrafast Electron Dynamics of PbS Nanoparticles with Different Surface Capping. *J. Phys. Chem. B* **2000**, *104*, 11598.
27. Ai, X.; Guo, L.; Zou, Y.; Li, Q.; Zhu, H. The Effect of Surface Modification on Femtosecond Optical Kerr Effect of PBS Nanoparticles. *Mater. Lett.* **1999**, *38*, 131.
28. Yang, J. P.; Qadri, S. B.; Ratna, B. R. Structural and Morphological Characterization of PbS Nanocrystallites Synthesized in the Bicontinuous Cubic Phase of a Lipid. *J. Phys. Chem.* **1996**, *100*, 17255.
29. Lipovskii, A.; Kolobkova, E.; Petrikov, V.; Kang, I.; Olkhovets, A.; Krauss, T.; Thomas, M.; Silcox, J.; Wise, F.; Shen, Q.; Kycia, S. Synthesis and Characterization of PbSe Quantum Dots in Phosphate Glass. *Appl. Phys. Lett.* **1997**, *71*, 3406–3408.
30. Olkhovets, A.; Hsu, R.-C.; Lipovskii, A.; Wise, F. W. Size-Dependent Temperature Variation of the Energy Gap in Lead-Salt Quantum Dots. *Phys. Rev. Lett.* **1998**, *81*, 3539.
31. Wise, F. Lead Salt Quantum Dots: The Limit of Strong Quantum Confinement. *Acc. Chem. Res.* **2000**, *33*, 773–780.
32. Wehrenberg, B. L.; Wang, C. J.; Guyot-Sionnest, P. Interband and Intraband Optical Studies of PbSe Colloidal Quantum Dots. *J. Phys. Chem. B* **2002**, *106*, 10634–10640.
33. Fernée, M. J.; Thomsen, E.; Jensen, P.; Rubinsztein-Dunlop, H. *Nanotechnology* **2006**, *17*, 956–962.
34. Franceschetti, A. Structural and Electronic Properties of PbSe Nanocrystals from First Principles. *Phys. Rev. B* **2008**, *78*, 075418.
35. Lifshitz, E.; Brumer, M.; Kigel, A.; Sashchiuk, A.; Bashouti, M.; Sirota, M.; Galun, E.; Burshtein, Z.; Le Quang, A. Q.;

Ledoux-Rak, I.; Zyss, J. Stable PbSe/PbS and PbSe/$PbSe_xS_{1-x}$ Core−Shell Nanocrystal Quantum Dots and their Applications. *J. Phys. Chem. B* **2006**, *110*, 25356–25365.
36. An, J. M.; Califano, M.; Franceschetti, A.; Zunger, A. Excited-State Relaxation in PbSe Quantum Dots. *J. Chem. Phys.* **2008**, *128*, 164720.
37. Allan, G.; Delerue, C. Confinement Effects in PbSe Quantum Wells and Nanocrystals. *Phys. Rev. B* **2004**, *70*, 245321.
38. Peterson, J. J.; Krauss, T. D. Fluorescence Spectroscopy of Single Lead Sulfide Quantum Dots. *Nano Lett.* **2006**, *6*, 510–514.
39. Fernée, M. J.; Jensen, P; Rubinsztein-Dunlop, H. Origin of the Large Homogeneous Line Widths Obtained from Strongly Quantum Confined PbS Nanocrystals at Room Temperature. *J Phys. Chem. C* **2007**, *111*, 4984–4989.
40. Fernée, M. J.; Jensen, P; Rubinsztein-Dunlop, H. Unconventional Photoluminescence Upconversion from PbS Quantum Dots. *Appl. Phys. Lett.* **2007**, *91*, 043112.
41. Harbold, J. M.; Wise, F. W. Photoluminescence Spectroscopy of PbSe Nanocrystals. *Phys. Rev. B* **2007**, *76*, 125304.
42. An, J. M.; Franceschetti, A.; Zunger, A. Pauli Blocking *versus* Electrostatic Attenuation of Optical Transition Intensities in Charged PbSe Quantum Dots. *Phys. Rev. B* **2007**, *76*, 161310.
43. Crooker, S. A.; Barrick, T.; Hollingsworth, J. A.; Klimov, V. I. Multiple Temperature Regimes of Radiative Decay in CdSe Nanocrystal Quantum Dots: Intrinsic Limits to the Dark-Exciton Lifetime. *Appl. Phys. Lett.* **2003**, *82*, 2793.
44. Rinnerbauer, V.; Egelhaaf, H. J.; Hingerl, K.; Zimmer, P.; Werner, S.; Warming, T.; Hoffmann, A.; Kovalenko, M.; Heiss, W.; Hesser, G.; Schaffler, F. Energy Transfer in Close-Packed PbS Nanocrystal Films. *Phys. Rev. B* **2008**, *77*, 085322.
45. Wuister, S. F.; van Houselt, A.; de Mello Donega, C.; Vanmaekelbergh, D.; Meijerink, A. Temperature Antiquenching of the Luminescence from Capped CdSe Quantum Dots. *Angew. Chem., Int. Ed.* **2004**, *43*, 3029–3033.
46. Hautman, J.; Klein, M. L. Molecular Dynamics Simulation of the Effects of Temperature on a Dense Monolayer of Long-Chain Molecules. *J. Chem. Phys.* **1990**, *93*, 7483.
47. Mielczarski, J. A.; Mielczarski, E. Determination of the Molecular-Orietation and Thickness of Self-Assembled Monolayers of Oleate on Apatite by FTIR Reflection Spectroscopy. *J. Phys. Chem.* **1995**, *99*, 3206–3217.